JOURNAL OF CHEMICAL & ENGINEERING DATA

ARTICLE

pubs.acs.org/jced

Equilibrated Interfacial Tension Data of the CO_2−Water System at High Pressures and Moderate Temperatures

Prem Kumar Bikkina,*[,†] O. Shoham,[†] and R. Uppaluri[‡]

[†]McDougall School of Petroleum Engineering, The University of Tulsa, Tulsa, Oklahoma 74104, United States

[‡]Department of Chemical Engineering, Indian Institute of Technology Guwahati, Guwahati, Assom 781039, India

ABSTRACT: This work presents interfacial tension (IFT) data for the CO_2−water system in the pressure and temperature range of (1.48 to 20.76) MPa and (298.15 to 333.15) K. The IFT evaluation is carried out using the pendant drop method. Inaccuracies observed in the literature such as consideration of pure phase densities and short presaturation time durations have been avoided by utilizing saturated phase densities and long presaturation time durations. The water-rich phase density is evaluated using a literature correlation, and the CO_2-rich phase density is evaluated using equation-of-state modeling approach. Also, presaturation times were extended up to 24 h to obtain equilibrated IFT data for the CO_2−water system. It is observed that the IFT reduces with pressure when the CO_2-rich phase is a gas at both subcritical and supercritical temperatures. Further, the IFT values reached a plateau at about 23 $mN \cdot m^{-1}$ at higher pressures (13.89 to 20.79 MPa) and for the entire temperature range. A predominant buoyancy effect is observable at higher pressures due to the reduction in phase density differences. Comparatively, the evaluated IFT data trends are about (5 to 7) $mN \cdot m^{-1}$ lower at high pressures than those reported in most of the literature.

1. INTRODUCTION

Saline aquifers are considered as one of the important host sites for carbon sequestration as they are ubiquitous and provide enormous volumes for sequestering large amounts of anthropogenic CO_2. For a safe and efficient sequestration process, an accurate representation of interfacial tension (IFT) and contact angles that strongly influence the relative permeability and capillary pressure is essential.[1] Further, both IFT and contact angle data trends during injection and postinjection periods are of paramount relevance.[2]

To date, a good number of experimental investigations addressed the measurement of IFT of the CO_2−water system at reservoir conditions.[3−13] Chun and Wilkinson[3] measured the IFT of CO_2−water−alcohol mixtures in the pressure range of (0.1 to 18.6) MPa and temperature range of (278.15 to 344.15) K using the capillary rise method. For the CO_2−water system, Hebach et al.[4,8] conducted IFT measurements using the pendant drop method in the pressure and temperature range of (0.1 to 20) MPa and (278 to 335) K, respectively. Emphasizing IFT measurements for prolonged time periods (to the order of 24 h), Tewes and Boury[5] carried out IFT measurement studies using the pendant drop method for pressures up to 9 MPa at 313.15 K. Akutsu et al.[6] conducted IFT measurements for water−CO_2 system at 318.15 K and up to 16.56 MPa. Chiquet et al.[7] observed that, at high pressures (>20 MPa), the IFT of the CO_2−water system is approximately independent of pressure, but it decreases very slowly with temperature. Sutjiadi et al.[11] reported that higher IFT values (about 3 $mN \cdot m^{-1}$) would be obtained when pure water densities are used instead of CO_2 saturated water densities. Bachu and Bennion[9,10,12] carried out extensive laboratory studies to measure the IFT of the CO_2−water system using the pendant drop method for a wide range of parametric choices of (2 to 27) MPa, (293.15 to 398.15) K, and (0 to 334) $g \cdot L^{-1}$ water salinity. A review of various adopted IFT measurement methods and the type of phase density values utilized by various investigators is given by Georgiadis et al.[13]

Though much data are available from various works,[3−14] the data reported by other research groups,[3−6,8,13] except for those provided by Chiquet et al.[7] and Bachu et al.,[9,10,12] used pure component phase densities instead of saturated phase densities. Since saturated phase densities have been adopted by recent researchers,[7,9,10,12] it is anticipated that the reported data shall be in good accord. However, when a thorough analysis has been carried out with the IFT data provided by Chiquet et al.[7] and Bachu et al.,[9,10,12] a greater disparity in the IFT data is prevalent for the data sets (Figure 1). From the figure, it is apparent that higher IFT data measurements were provided by Chiquet et al.[7] when compared to Bachu et al.[9,10,12] at higher pressures, and these deviations amounted to about 100 % variation. The prevalent disparities in these IFT data are bound to generate additional errors in reservoir site characterization and subsequent analysis. For the purpose of reservoir site characterization, IFT data obtained with long-term exposure to the CO_2−water system is required.

Possible reasons for disparities in the IFT data include errors propagated in the measurement method, the procedure itself, and the subsequent analysis. These include utilization of pure component phase densities,[3−6,8,13] incomplete saturation of the phases involved, smaller measurement times that refer to local equilibrium IFT values,[3,4,6−14] position of the thermocouple,[3] and so forth. In addition, appropriate calibration of the equipment and quality of the fluids used also affect the IFT data provided. Last but not the least, the clarity of the droplet picture is very critical to obtain reliable IFT data, if the method followed for the IFT measurement is a drop-shape analysis based method (e.g., pendant and sessile drop methods).

Received: March 29, 2011
Accepted: September 8, 2011
Published: September 21, 2011

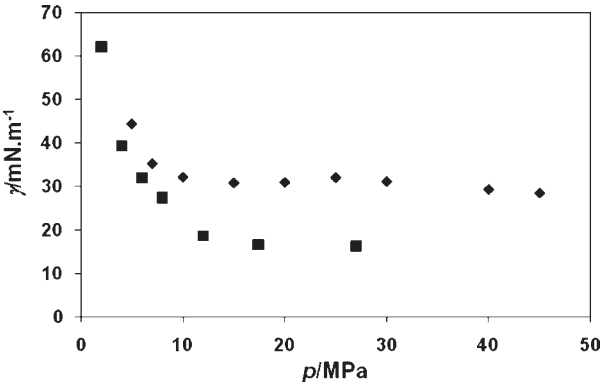

Figure 1. CO_2—water system IFT vs pressure data of ♦, Chiquet et al.;[7] and ■, Bachu et al.[12] at 308 K.

This work addresses the IFT measurement of the CO_2—water system at temperatures of (298.15 to 333.15) K and pressures of (1.48 to 20.79) MPa, respectively. Measurements are conducted for prolonged times of around 24 h to ensure equilibrium IFT values using the pendant drop method. Saturated phase densities are utilized for the evaluation of IFT data. An equation of state (EOS) modeling procedure given by Spycher et al.[15] is modified to evaluate the saturated CO_2-rich phase densities using first principles. The saturated water-rich phase densities were evaluated using a correlation developed by Hebach et al.[16] from their experimental data.

2. EVALUATION OF EQUILIBRIUM PHASE DENSITIES

Accurate saturated phase density values, for the CO_2—water system, are important not only to measure IFT between the phases but also to predict the multiphase flow behavior and segregation of the fluid phases in the sequestration zone. Hence, this work reports the efficacy of an integrated computer code that could generate both CO_2-rich and water-rich phase densities for the CO_2—water system.

The developed integrated computer code embedded the extended solubility model of Spycher et al.[15] and phase density correlation of Hebach et al.[16] to calculate CO_2-rich phase densities and water-rich phase densities, respectively.

Spycher et al.[15] developed a noniterative method to calculate mutual solubilities of the CO_2—water system in the range of (288.15 to 373.15) K and up to 60 MPa. They adopted an inverse modeling procedure to simultaneously determine the Redlich—Kwong parameters and aqueous solubility constants (as a function of temperature) for gaseous, liquid, and supercritical CO_2, by tuning the parameters using most of the previously published solubility data for the CO_2—water system. By doing so, they could reproduce mutual solubilities of water from (288.15 to 373.15) K and CO_2 from (285.15 to 383.15) K and up to 60 MPa within reasonable accuracy. Precisely, in this work, the Spycher et al.[15] methodology was used to predict mutual solubilities of the CO_2—water system, and then it has been extended to predict the saturated phase densities of the CO_2-rich phase.

Hebach et al.[16] developed a density correlation for the water-rich phase with their experimental data, measured by using a calibrated vibrating-tube mass flow meter with an uncertainty below 0.15 % and also with previously published literature data with uncertainties below 1 %. The pressure and temperature ranges of the correlation are (1 to 30) MPa and (284.15 to 333.15) K, respectively, and the quality of reproduction, within its experimental range of pressure and temperature, is 99.75 %.

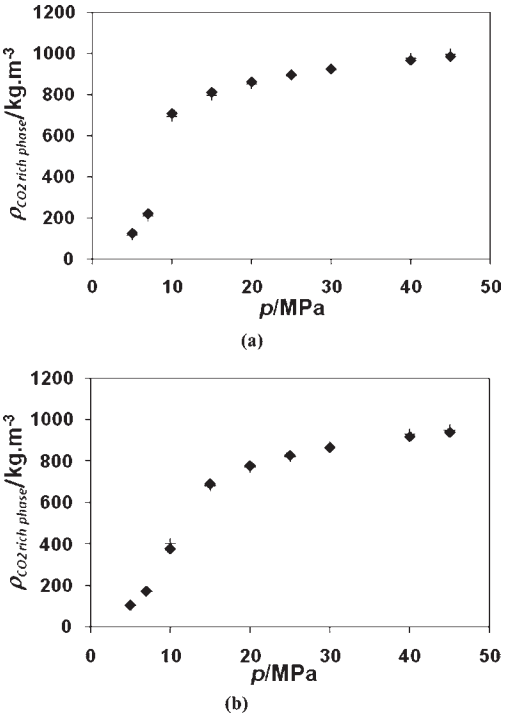

Figure 2. Comparison between ♦, experimental;[7] and +, predicted saturated phase density vs pressure data for the CO_2-rich phase of the CO_2—water system at (a) about 308 K and (b) about 323.5 K.

On the basis of the limits for the developed models in the literature, the integrated computer code is anticipated to provide fairly accurate phase densities within the pressure range of (1 to 30) MPa and temperature range of (288.15 to 333.15) K, given the fact that these parameter ranges correspond to the intersection conditions for both Spycher et al.[15] and Hebach et al.[16]

The predicted phase densities are compared (Figures 2 and 3) with the recently published experimental phase density data of Chiquet et al.,[7,14] and it is found that the experimental and predicted data are in good agreement. Also, it can be noted from Figure 3 that Hebach et al.[16] phase density correlation is also effective well beyond its intended pressure range (30 MPa).

In the recently published IFT data for CO_2—water system, Georgiadis et al.[13] conveyed that their data are based on pure component densities and possibilities to correct the data using saturated phase densities as recommended. Therefore, in this work, to visualize the competence of the data generated by the authors, the saturated phase densities computed in this work are compared with those provided by the authors and are summarized in Figure 4. It is evident from the figure that the differences in phase densities are significant at lower temperatures and higher pressures.

3. EXPERIMENTAL SECTION

3.1. Materials and Instruments. Laboratory grade CO_2 (99.99 mole percent purity) and ultra pure Millipore water (18.2 MΩ·cm) were used for all IFT measurements. The equipment used was a custom-made high pressure (69 MPa) and moderate temperature (450 K) sustainable IFT machine. The schematic of the experimental setup used for the IFT

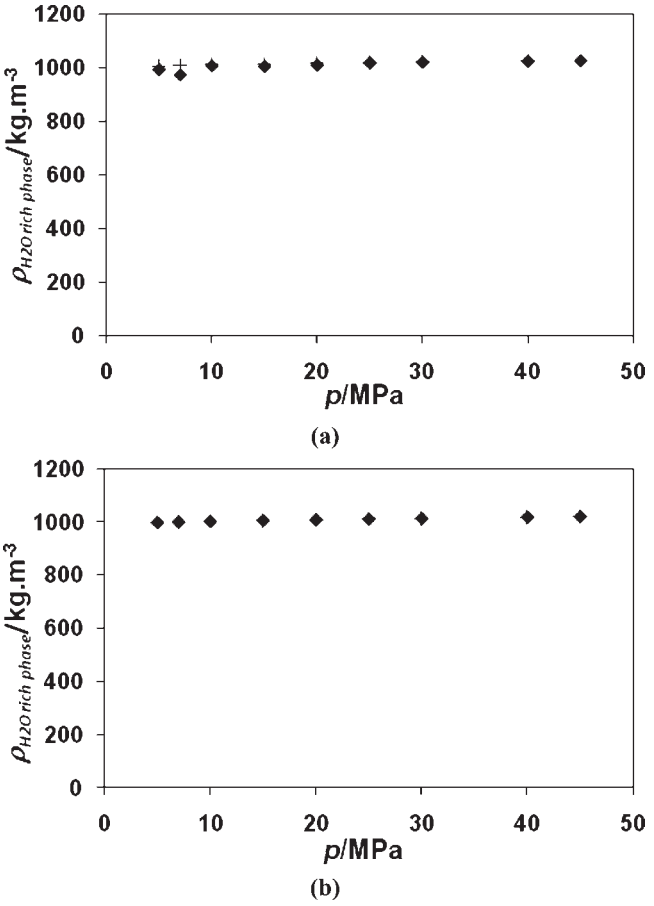

Figure 3. Comparison between ♦, experimental;[7] and +, predicted saturated phase density vs pressure data for the water-rich phase of the CO_2−water system at (a) about 308 K and (b) about 323.5 K.

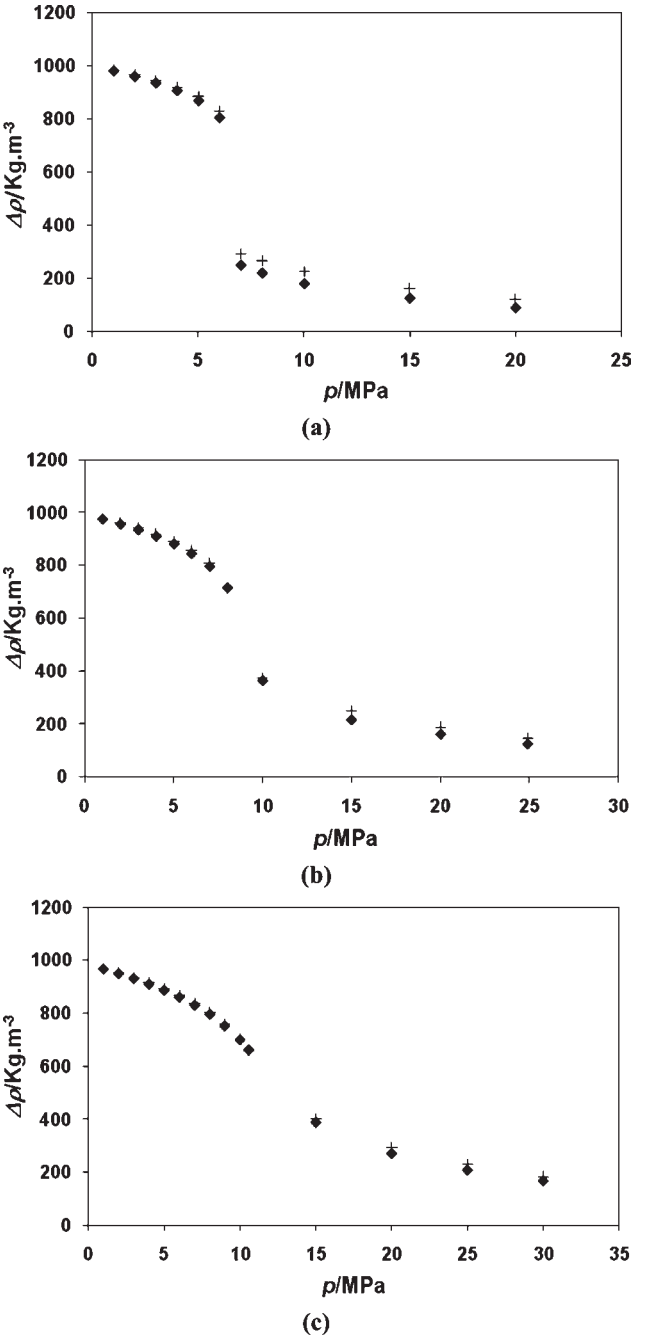

Figure 4. Comparison of predicted saturated phase density difference (+) of the CO_2−water system with Georgiadis et al.[13] pure component phase density difference (♦) data at (a) T = 297.8 K, (b) T = 312.8 K, and (c) T = 333.5 K.

measurements is given in Figure 5. The following subsections highlight important components of the experimental setup along with their functions.

3.1.1. IFT Cell. The IFT cell was purchased from Temco Division of Core Laboratories. Primarily, it constitutes a 316 stainless steel cell, two thick borosilicate glass windows, and two stainless steel needles. The 316 stainless steel cell with an approximate volume of $25 \cdot 10^{-6}$ m^3 has four ports, for fluid inlet, fluid outlet, temperature, and pressure measurements. The cell is wrapped with two stripper heaters with a temperature controller (WATLOW Series 989, Omega "K" type thermo couple). The borosilicate glass windows facilitate observation of the CO_2-saturated water drop, which is surrounded with water-saturated CO_2. The glass windows are fixed parallel to one another using high-pressure, high-temperature, and CO_2-compatible o-rings and seals (Formulated AFLAS from Seals Eastern, Inc.). When Viton and Buna seals were used initially, explosive decompression of the seals was observed during depressurization of the IFT cell. Among the two stainless steel needles (outer diameter $1.6 \cdot 10^{-3}$ m, inner diameter $0.78 \cdot 10^{-3}$ m), one is used to make drops for the pendant drop method, and the other is used for the sessile drop IFT measurement and to hold the base that supports the substrate for contact angle measurements.

3.1.2. Fluid Saturation and Circulation System. The fluid saturation and circulation system primarily consists of syringe pumps, saturation vessels, and stainless steel tubing. Two pulsation-free syringe pumps (Teledyne ISCO model 260D) with a controller (D-series) are used to pump supercritical fluid, droplet phase fluid, and external phase fluid. A third pump (Eldex, Optos Seiries, model 2) was used for cleaning the IFT cell using acetone and Millipore water. After water flushing, the view cell was flushed with CO_2 for about 5 min to ensure that air was completely displaced from the view cell. It was also used to make a stable drop, during the drop-making step. Two 316 stainless steel saturation vessels (maximum working pressure of 69 MPa at 450 K) are used to presaturate the droplet phase fluid and the external phase fluid at

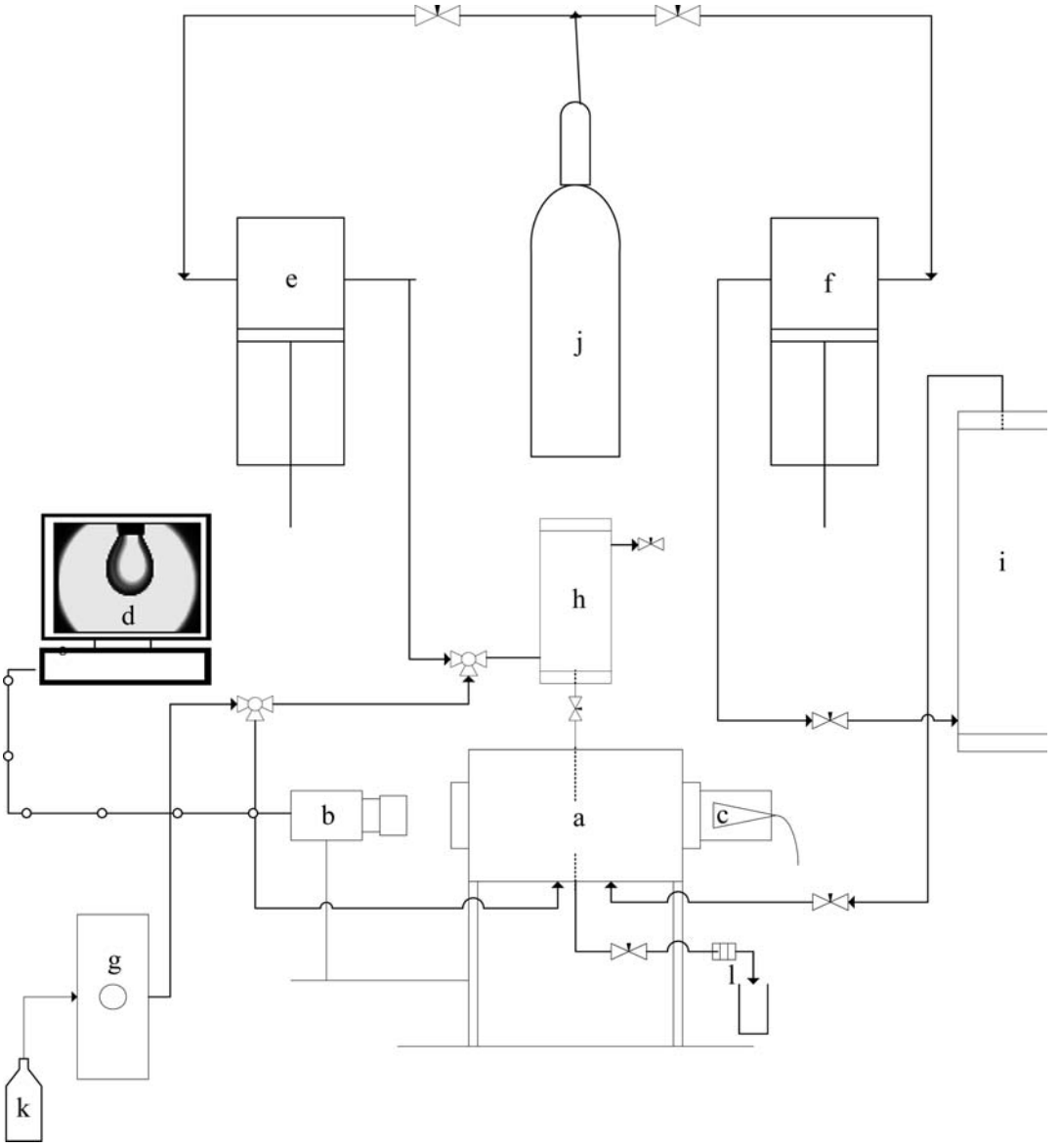

Figure 5. Schematic of the experimental setup used for IFT measurements. (a) IFT cell, (b) charge-coupled device (CCD) camera, (c) background light source, (d) computer, (e and f) syringe pumps, (g) reciprocating piston pump, (h and i) saturation vessels for the water-rich and CO_2-rich phases, respectively, (j) CO_2 cylinder, (k) Millipore-water can, and (l) back pressure regulator.

the desired pressure. The 316 stainless steel tubing (maximum working pressure of 69 MPa at 450 K) is used to connect the above-mentioned components to facilitate a high pressure fluid saturation and circulation loop.

3.1.3. Drop Image Analysis. The drop image analysis is carried out using a CCD camera and a background light source to record the drop image. Further, Rame-Hart's dropimage Advanced v2.3 software installed on a personal computer was used for image analysis.

3.2. Experimental Procedure. Before each measurement, the IFT cell was flushed with Millipore water and calibrated using the same needle used to make the drop. For the calibration step, the needle should cover the entire vertical visual length of the camera focus, whereas during the actual IFT measurement the needle tip should be in the middle or top of the camera focus area so that entire drop is clearly visible in the frame. The capillary needle could be moved vertically up and down even when the cell is under pressure. The calibration constants (aspect ratio) were between 0.9997 and 1.000 (if the calibration constant is one/very close to one, then the calibration is rendered perfect). The surface tension of water was measured to confirm the reliability of the measurements, and the values were found to match with the literature values.

To carry out the measurement, CO_2 and water were saturated in the saturation vessels at the required pressure before they were admitted into the IFT cell. First the external phase, which was water-saturated CO_2, was slowly admitted into the cell using a syringe pump (component f in Figure 5). When the external phase is at the required pressure, a CO_2-saturated water droplet was made at the tip of the capillary needle using the third pump (component g in Figure 5). When a sufficiently big and stable drop was obtained, IFT measurements were carried out by making images of the drop using the CCD camera and digitalizing the drop shape. The IFT data was obtained by matching the

Table 1. IFT Measurements of the CO_2−Water System and Corresponding Phase Densities Utilized

P	T		$\rho_{CO_2\text{-RP}}$	$\rho_{water\text{-RP}}$	γ
MPa	K	CO_2-RP[a]	kg·m^{-3}	kg·m^{-3}	mN·m^{-1}
1.48	298.15	G	28.4	1002.0	59.66 ± 0.14
2.86	298.15	G	60.0	1006.0	50.25 ± 0.06
4.24	298.15	G	100.0	1010.0	44.09 ± 0.08
5.62	298.15	G	158.9	1013.0	35.95 ± 0.08
8.38	298.15	L	756.3	1015.0	25.65 ± 0.17
10.44	298.15	L	795.6	1016.0	25.15 ± 0.07
13.89	298.15	L	843.0	1018.0	24.85 ± 0.08
17.34	298.15	L	878.4	1020.0	24.9 ± 0.07
20.79	298.15	L	907.1	1022.0	25 ± 0.06
1.48	313.15	G	26.6	995.2	57.52 ± 0.45
2.86	313.15	G	55.4	998.6	51.32 ± 0.09
4.24	313.15	G	89.7	1002.0	47.50 ± 0.16
5.62	313.15	G	133.1	1004.0	42.17 ± 0.12
8.38	313.15	SC	448.6	1007.0	22.23 ± 0.21
10.44	313.15	SC	649.9	1009.0	22.16 ± 0.28
13.89	313.15	SC	739.3	1010.0	23.33 ± 0.20
17.34	313.15	SC	792.8	1012.0	23.41 ± 0.2
20.79	313.15	SC	832.4	1014.0	25.07 ± 0.22
1.48	323.15	G	25.6	990.1	59.16 ± 0.17
2.86	323.15	G	52.8	992.9	54.23 ± 0.39
4.24	323.15	G	84.3	995.4	50.14 ± 0.27
5.62	323.15	G	122.3	997.5	44.15 ± 0.04
8.38	323.15	SC	242.7	1001.0	31.18 ± 0.08
10.44	323.15	SC	483.4	1003.0	23.05 ± 0.11
13.89	323.15	SC	656.1	1005.0	22.74 ± 0.32
17.34	323.15	SC	729.4	1007.0	24.27 ± 0.37
20.79	323.15	SC	778.9	1008.0	23.5 ± 0.14
1.48	333.15	G	24.60	984.6	60.69 ± 0.07
2.86	333.15	G	50.50	986.8	55.39 ± 0.23
4.24	333.15	G	79.80	988.8	51.15 ± 0.12
5.62	333.15	G	113.9	990.7	45.84 ± 0.20
8.38	333.15	SC	207.5	993.8	35.83 ± 0.16
10.44	333.15	SC	328.8	995.7	31.70 ± 0.23
13.89	333.15	SC	559.7	998.6	23.36 ± 0.15
17.34	333.15	SC	661.0	1000.0	23.58 ± 0.32
20.79	333.15	SC	722.9	1002.0	22.8 ± 0.29

[a] RP− rich phase, G − gas, L − liquid, SC − supercritical.

drop profile (axisymmetric drop shape analysis, ADSA) to the solutions of the Laplace equation. A detailed explanation of the ADSA method can be found elsewhere.[7,17]

Since both of the phases were saturated at room temperature and experimental pressure, it was required to keep them in contact for some more time to reach equilibrium at the experimental temperature that was maintained in the IFT cell using stripper heaters and a temperature controller. About ($1 \cdot 10^{-6}$ to $2 \cdot 10^{-6}$) m^3 of water was maintained at the bottom of the cell to ensure phase equilibrium between the droplet and the external phase fluids inside the IFT cell. To ensure equilibrium IFT values, the IFT measurements at each pressure and temperature combination were carried out for the prolonged time duration of 24 h. The IFT measurements for the CO_2−water system were carried out in the temperature and pressure range of (298.15 to 333.15) K and (1.48 to 20.79) MPa, respectively. The uncertainties of the temperature and pressure measuring instruments were about ± 0.1 % (linear accuracy). For each experiment that lasted between (12 to 24) h, the mean IFT values (and standard deviation values) are evaluated using the last 10 readings obtained with 15 min of time intervals. The mean IFT data along with standard deviations are presented in Table 1.

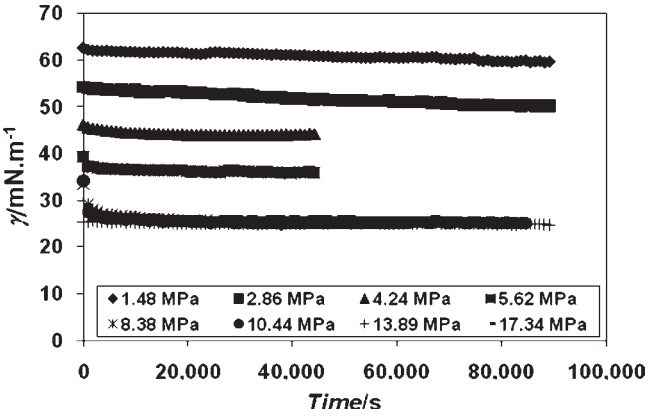

Figure 6. Variation of IFT with time and pressure for the CO_2−water system at 298.15 K.

4. RESULTS AND DISCUSSION

4.1. Effect of Time. Figure 6 presents the IFT variation with time at various pressures for the CO_2−water system. Though experimental observations were carried out for about 24 h, the aging effect as reported by Hebach et al.[4,8] that indicates a sudden decrease in the IFT values after around 10 min was not observed in our case. The possible reasons for the observation of the aging effect by Hebach et al.[4,8] are that (a) local equilibrium IFT values might have been considered, (b) tiny leakage of the external phase fluid from the IFT cell during measurement may occur, and (c) dissolution of surface active components of the seal material in the liquid/supercritical CO_2 when the seals used are not compatible with the operating conditions of the system. In this work, the temperature difference between the view cell and the saturation vessel is anticipated to be the major cause for the time dependence and long equilibration times.

4.2. Effect of Pressure on IFT. Figure 7 presents photographs of the CO_2 saturated water droplets in the water-saturated CO_2 at pressures ranging from (1.48 to 20.79) MPa at 298.15 K. It can be observed from the figure that, as pressure increases, buoyancy effects become predominant. This is due to the reason that the phase density difference between the external and the droplet phases decreases with increasing pressure and thus gives rise to larger droplets before they detach from the needle at higher pressures. Also, the figure depicts two IFT data measurements at 10.44 MPa (1500 psig). The primary purpose of these two measurements is to ensure that the water level in the system does not have any effect on the IFT data. Further, IFT data at 10.44 MPa were repeated, and the data obtained were reproducible with a variation of only 0.2 mN·m^{-1}.

In conjunction with the reported IFT data, the effect of pressure on the mean IFT at various temperatures is presented in Figure 8a,b. As shown in Figure 8a, the obtained IFT values are in close agreement with those presented in the literature.

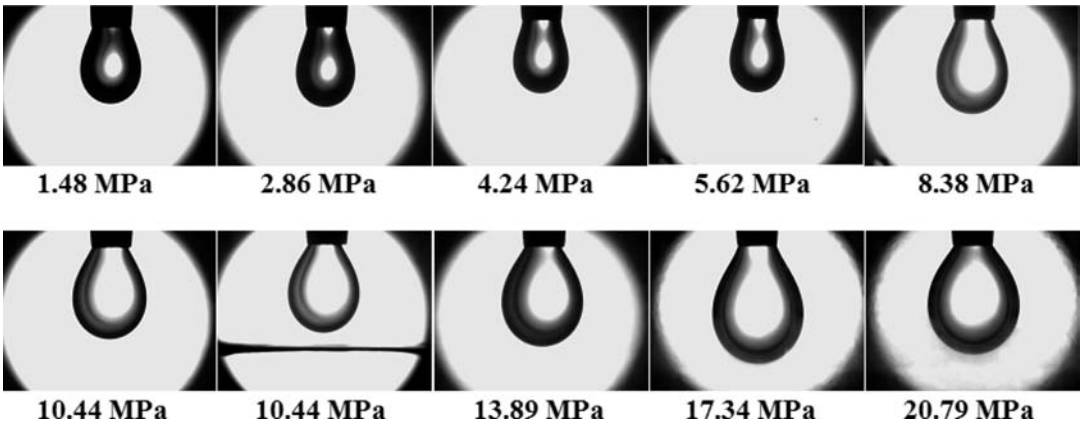

Figure 7. Photographs of CO_2-saturated water droplets in water-saturated CO_2 at 298.15 K and various pressures.

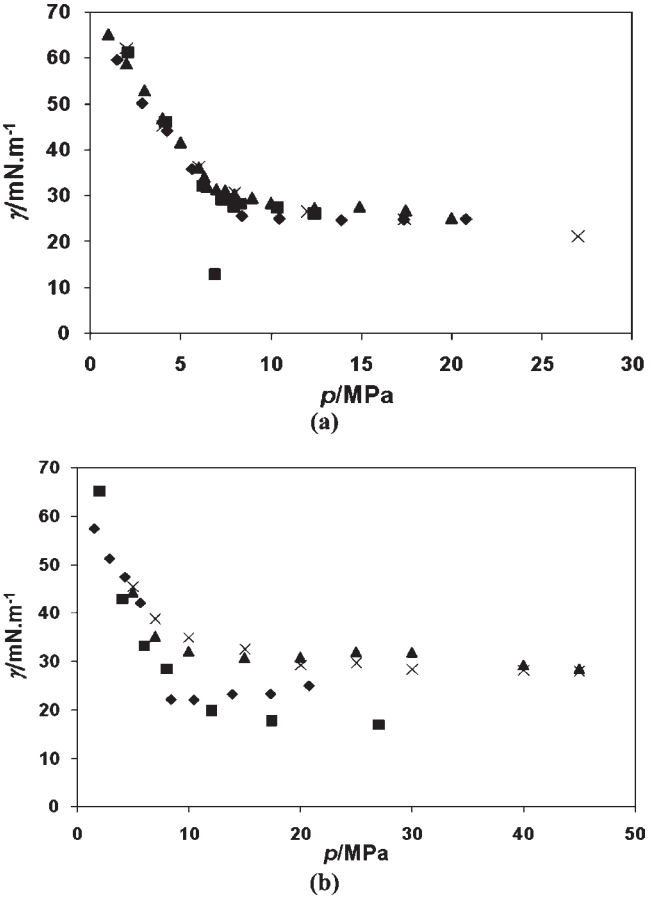

Figure 8. (a) Comparison of obtained IFT data for the CO_2−water system at 298.15 K (♦) with the IFT data presented by ■, Chun et al.;[3] ▲, Hebach et al.;[4] ×, Bachu et al.[9] (b) Comparison of obtained IFT data for the CO_2−water system at 313.15 K (♦) with the IFT data provided by ■, Bachu et al.[9] at 314.15 K; Chiquet et al.[7] at ▲, 308 K and ×, 323.5 K.

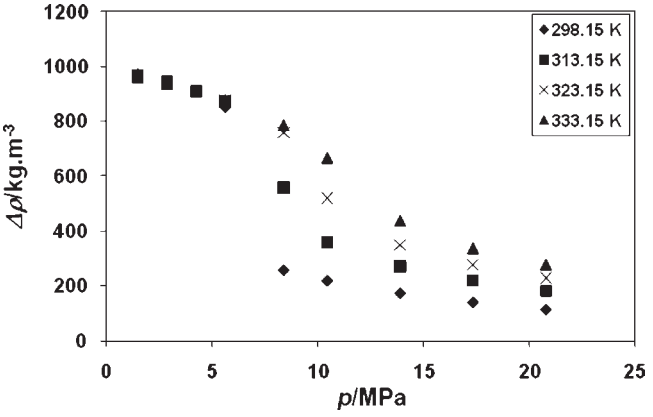

Figure 9. Variation of the phase density difference with pressure and temperature for the CO_2−water system.

However, the IFT values reported in this work are slightly smaller than that of the other literature values[3,7−10,12] at all pressures. This is due to the long equilibrating periods during presaturation and actual measurement, which can be visualized in Figure 6. It can be also seen in Figure 8a that the decreasing IFT trend with pressure followed a perfect straight line in the low pressure range (gaseous CO_2-rich phase) and the IFT values with increasing pressure become nearly constant (horizontal line) of pressure when the CO_2-rich phase is liquefied (i.e., at high pressures), even though the corresponding phase density difference decreases continuously (Figures 4a−c and 9).

Also, some explanation has been provided by Hebach et al.[4,8] for the deviation of the IFT value of Chun et al.[3] at 6.89 MPa in Figure 8a. The possible reasons are (a) placing the thermocouple in the insulation instead of external phase fluid (inside the cell) and (b) drastic phase density change near to the dew-point pressure (phase changing pressure at a given temperature), due to which even a very small error in the pressure measurement would cause a big change in the CO_2-rich phase/CO_2-phase density value.

A comparative assessment of IFT data obtained in this work with those presented by Bachu et al.[9,10,12] and Chiquet et al.[7] is pictorially presented in Figure 8b. It is evident from the figure that, at lower pressures (< 8 MPa), the IFT data in this work are in good agreement with that evaluated by Bachu et al. and Chiquet et al. However, at higher pressures, the data obtained in this work at 313.15 K deviated significantly from that obtained by Bachu et al.[9,10,12] at 314.15 K. A deviation of about 32 % is evident at the highest system pressure value, and this is attributed to both inaccuracy in density evaluations and short duration IFT measurements. Thus, this work attempts to provide reliable data for the purpose of efficient sequestration studies in the near future. Also, it is important to note in the same figure that the data

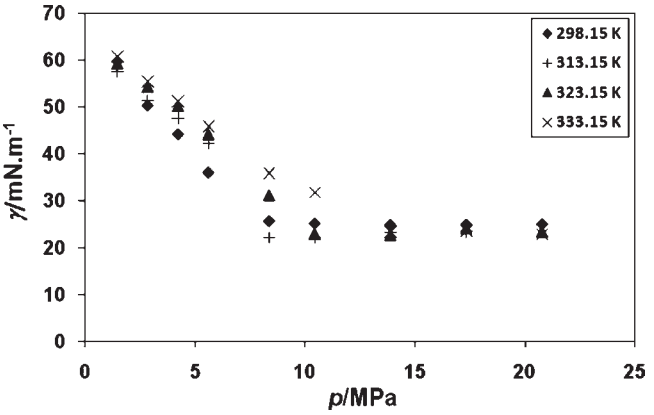

Figure 10. IFT isotherms for the CO_2−water system at various pressures.

reported by Chiquet et al.[7] matched at two different temperatures, (308.15 and 323.15) K.

4.3. Effect of Temperature on IFT. Figure 10 presents four isotherms of pressure versus IFT for water-saturated CO_2 (gaseous, liquid, and supercritical) and CO_2-saturated water system. It is observed that, above the supercritical temperature (304.63 K[18]) of the CO_2−water system and when the CO_2-rich phase is a gas, the IFT decreased sharply with pressure and increased with the temperature. However, in the high-pressure region and above the supercritical temperature, within the range of our experimental pressure and temperature, IFT is almost constant with both pressure and temperature.

Very similar trends were observed by Hebach et al.,[4,8] but their IFT values are higher by about 5 $mN \cdot m^{-1}$ than the values obtained in this work. Sutjiadi-Sia et al.[11] have shown that higher IFT values of about 3 $mN \cdot m^{-1}$ compared to the actual would be obtained if pure water density values are utilized in the place of CO_2-saturated water density. The same could be the cause for the deviation between our IFT data and the Hebach et al.[4,8] IFT data. Also, a possible consideration of local equilibrium values could be another reason as it is mentioned earlier. Bachu et al.[9,10,12] reported that, above the supercritical temperature of the CO_2−water system, IFT increased with temperature both in the gaseous (low pressure) and liquid/supercritical (high pressure) CO_2-rich phase conditions, whereas Chun et al.[3] mentioned that IFTs of the CO_2−water system decrease linearly with both temperature and pressure in the low-pressure range (gaseous CO_2), but the IFT was mostly independent of pressure at the high-pressure (supercritical CO_2) region. Chiquet et al.[7] observed that, at high pressures (> 20 MPa), the IFT of CO_2−water system is approximately independent of pressure, but it decreases very slowly with temperature. These data trends are totally in disagreement with the trends observed by Bachu et al.[9,10,12] Chalbaud et al.[1,19] and Aggelopoulos et al.[20] IFT data trends, with pressure and temperature, are similar to our data trends despite the fact that their systems are CO_2-aqueous sodium chloride solution and CO_2-aqueous calcium chloride solution, respectively. Both Bachu et al.[9,10,12] and Chalbaud et al.[1,19] concluded that the IFT of the CO_2−brine system increases with increasing brine salinity and is the consequence of decreasing CO_2 solubility in the brine as its salinity increases. Considering this fact and the IFT data of the Chalbaud et al.[1,19] and Aggelopoulos et al.,[20] IFTs of the CO_2−water system, when the CO_2-rich phase is supercritical, must be less than 25 $mN \cdot m^{-1}$ (the Chalbaud et al.[1,19]

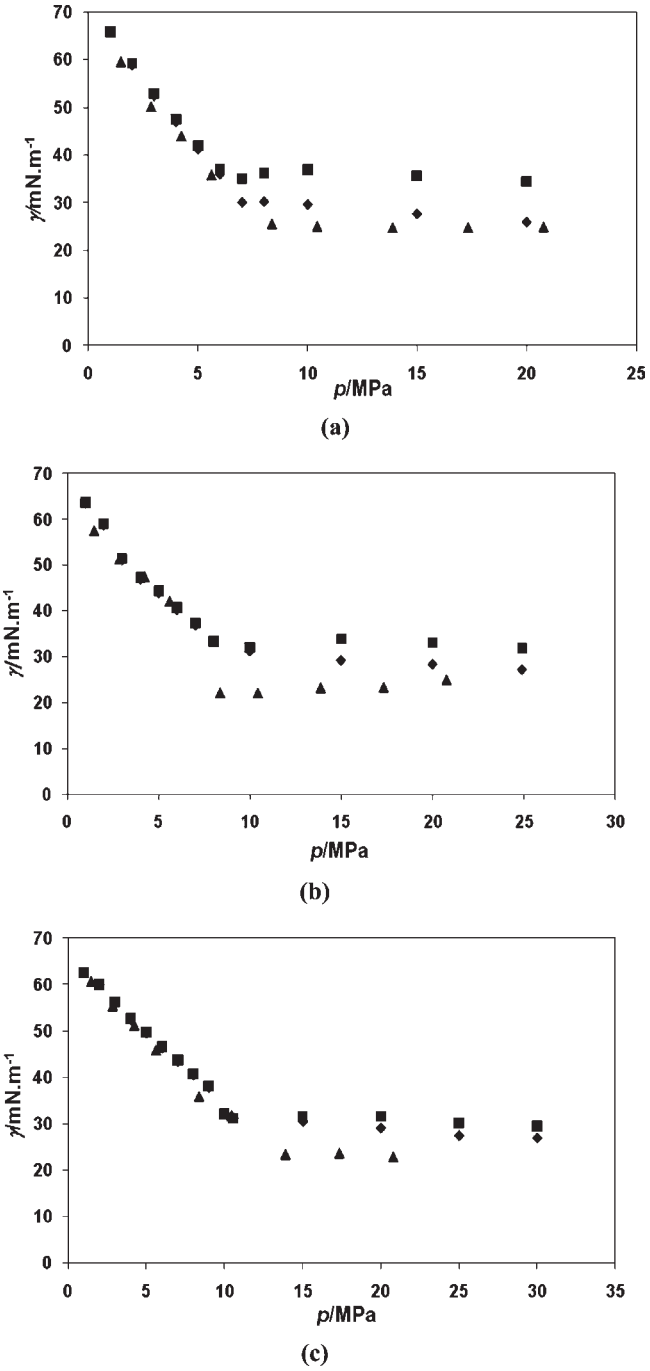

Figure 11. Comparison of obtained IFT isotherms for the CO_2−water system at various temperatures [(a) $T \approx 298$ K; (b) $T \approx 313$ K; (c) $T \approx 333$ K] and pressures with corresponding literature data. ▲, Data legends correspond to measured data; ♦, IFT data provided by Geordiagis et al.[13] based on pure component phase densities; and ■, corrected IFT data of Geordiagis et al.[13]

minimum IFT was around 25 $mN \cdot m^{-1}$ and it increased with the salinity of the brine), and that confirms the reliability of the present work.

In comparison with the reported data at various temperatures, the IFT data determined in this work is pictorially represented in Figure 11a−c. The literature data correspond to IFT data evaluated using pure component phase densities (Georgiadis et al.[13]) and

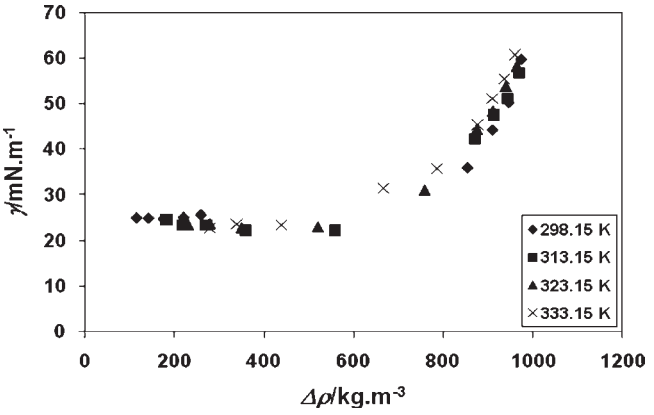

Figure 12. Effect of the phase density difference on IFT for the CO_2−water system at various temperatures.

IFT data of the authors evaluated using saturated phase densities. It is evident from these figures that, as temperature increases, the IFT data trends corresponding to the literature values become close to one another. This is due to the fact that at higher temperatures the assumption of regarding pure component phase densities as saturated phase densities would be more appropriate. Also, it is interesting to note that the IFT data obtained in this work are located slightly below the reported IFT data trends at lower pressures and significantly lower than that reported at higher pressures. It is further interesting to note that the corrected IFT data of Georgiadis et al.[13] using saturated phase densities also deviated from the corresponding literature values as well as the values reported in this work. In summary, these deviations in the IFT data are possibly due to the larger deviations of saturated phase densities at high pressures and low temperatures (Figure 4a−c).

The equilibrated mean IFT variation with a variation in phase density differences is illustrated in Figure 12. The figure indicates a characteristic nearly invariant IFT from a phase density difference up to 600 $kg \cdot m^{-3}$ and a linear variation in IFT from a phase density difference values up to 973.6 $kg \cdot m^{-3}$. Very similar trends were reported for IFT data trends reported by Chalbaud et al.[1,19] More precisely, in our work we have observed that an increase in temperature enabled a maximum variation in the IFT values by (5 to 7) $mN \cdot m^{-1}$ above a phase density difference value of 600 $kg \cdot m^{-3}$.

5. CONCLUSIONS

Experimental IFT data for the CO_2−water system are generated, using the pendant drop (ADSA) method, at pressures and temperatures relevant to general carbon sequestration conditions. Both the droplet phase and the external phase fluids are presaturated for more than 24 h (as the pressure increases, saturation times are increased, and by the time it reaches the highest experimental pressure at a given temperature, both the fluids are saturated for more than 7 days) to ensure the attainment of phase equilibrium by complete phase saturation. Experiments are conducted for extended times, of around 24 h, to guarantee global equilibrium IFT values. All possible causes that contribute to erroneous IFT measurements have been taken care to obtain accurate IFT values for the CO_2−water system, as reliable IFT data is required for the evaluation of reservoir capacities to hold huge quantity of manmade CO_2 emissions.

It is observed that IFT decreases with pressure when the CO_2-rich phase is a gas, at both subcritical and supercritical experimental temperatures. On the other hand, IFTs are observed to be independent of both pressure and temperature when the CO_2-rich phase is either a liquid or a supercritical fluid. In the low-pressure region (gaseous CO_2-rich phase) IFT increased with temperature at a given pressure, and at very low pressures, all of the isotherms asymptotically approach one another. In summary, the reported equilibrated IFT data trends based on saturated phase density data are anticipated to provide more reliable data for sequestration research in the near future.

AUTHOR INFORMATION

Corresponding Author

*E-mail: prem-bikkina@utulsa.edu. Phone: 001-918-619 2413.

ACKNOWLEDGMENT

The authors convey their sincere acknowledgements to Jerry Schoeffler, Technican at McDougall School of Petroleum Engineering, University of Tulsa for extending support towards the fabrication of the custom-made high-pressure high-temperature IFT/contact angle experimental setup.

REFERENCES

(1) Chalbaud, C.; Robin, M.; Lombard, J. M.; Martin, F.; Egermann, P.; Bertin, H. Interfacial tension measurements and wettability evaluation for geological CO_2 storage. *Adv. Water Resour.* **2009**, *32*, 98–109.

(2) Li, Z.; Dong, M.; Li, S.; Huang, S. CO_2 sequestration in depleted oil and gas reservoirs—caprock characterization and storage capacity. *Energy Convers. Manage.* **2006**, *47*, 1372–1382.

(3) Chun, B.-S.; Wilkinson, G. T. Interfacial tension in high-pressure carbon dioxide mixtures. *Ind. Eng. Chem. Res.* **1995**, *34*, 4371–4377.

(4) Hebach, A.; Oberhof, A.; Dahmen, N.; Kogel, A.; Ederer, H.; Dinjus, E. Interfacial Tension at Elevated Pressures—Measurements and Correlations in the Water + Carbon Dioxide System. *J. Chem. Eng. Data* **2002**, *47*, 1540–1546.

(5) Tewes, F.; Boury, F. Formation and Rheological Properties of the Supercritical CO_2−Water Pure Interface. *J. Phys. Chem. B* **2005**, *109*, 3990–3997.

(6) Akutsu, T.; Yamaji, Y.; Yamaguchi, H.; Watanabe, M.; Smith, R. L., Jr.; Inomata, H. Interfacial tension between water and high pressure CO_2 in the presence of hydrocarbon surfactants. *Fluid Phase Equilib.* **2007**, *257*, 163–168.

(7) Chiquet, P.; Daridon, J.-L.; Broseta, D.; Thibeau, S. CO_2/water interfacial tensions under pressure and temperature conditions of CO_2 geological storage . *Energy Convers. Manage.* **2007**, *48*, 736–744.

(8) Kvamme, B.; Kuznetsova, T.; Hebach, A.; Oberhof, A.; Lunde, E. Measurements and modelling of interfacial tension for water + carbon dioxide systems at elevated pressures. *Comput. Mater. Sci.* **2007**, *38*, 506–513.

(9) Bachu, S.; Bennion, D. B. Interfacial Tension between CO_2, Freshwater, and Brine in the Range of Pressure from (2 to 27) MPa, Temperature from (20 to 125) °C, and Water Salinity from (0 to 334000) $mg \cdot L^{-1}$. *J. Chem. Eng. Data* **2008**, *54*, 765–775.

(10) Bennion, D. B.; Bachu, S. In *SPE Annual Technical Conference and Exhibition*; Society of Petroleum Engineers: Denver, CO, 2008.

(11) Sutjiadi-Sia, Y.; Jaeger, P.; Eggers, R. Interfacial phenomena of aqueous systems in dense carbon dioxide. *J. Supercrit. Fluids* **2008**, *46*, 272–279.

(12) Bachu, S.; Bennion, D. B. Dependence of CO_2-brine interfacial tension on aquifer pressure, temperature and water salinity. *Energy Procedia* **2009**, *1*, 3157–3164.

(13) Georgiadis, A.; Maitland, G.; Trusler, J. P. M.; Bismarck, A. Interfacial Tension Measurements of the (H_2O + CO_2) System at Elevated Pressures and Temperatures. *J. Chem. Eng. Data* **2010**, *55*, 4168–4175.

(14) Chiquet, P.; Daridon, J.-L.; Broseta, D.; Thibeau, S. Erratum to the paper "CO_2/water interfacial tensions under pressure and temperature and conditions of CO2 geological storage", by Pierre Chiquet, Jean-Luc Daridon, Daniel Broseta, Sylvain Thibeau, published in Energy Convers. Manage. 48 (2007) 736−44. *Energy Convers. Manage.* **2009**, *50*, 431.

(15) Spycher, N.; Pruess, K.; Ennis-King, J. CO_2-H_2O mixtures in the geological sequestration of CO_2. I. Assessment and calculation of mutual solubilities from 12 to 100 °C and up to 600 bar. *Geochim. Cosmochim. Acta* **2003**, *67*, 3015–3031.

(16) Hebach, A.; Oberhof, A.; Dahmen, N. Density of Water + Carbon Dioxide at Elevated Pressures: Measurements and Correlation. *J. Chem. Eng. Data* **2004**, *49*, 950–953.

(17) Arashiro, E. Y.; Demarquette, N. R. Use of the pendant drop method to measure interfacial tension between molten polymers. *Mater. Res.* **1999**, *2*, 23–32.

(18) Wendland, M.; Hasse, H.; Maurer, G. Experimental Pressure−Temperature Data on Three- and Four-Phase Equilibria of Fluid, Hydrate, and Ice Phases in the System Carbon Dioxide−Water. *J. Chem. Eng. Data* **1999**, *44*, 901–906.

(19) Chalbaud, C. A.; Robin, M.; Egermann, P. In *SPE Annual Technical Conference and Exhibition*; Society of Petroleum Engineers: San Antonio, TX, 2006.

(20) Aggelopoulos, C. A.; Robin, M.; Perfetti, E.; Vizika, O. CO_2/$CaCl_2$ solution interfacial tensions under CO_2 geological storage conditions: Influence of cation valence on interfacial tension. *Adv. Water Resour.* **2010**, *33*, 691–697.